ANALYTICAL AND NUMERICAL MODELS FOR PREDICTING UNFOLDING FAILURE IN COMPOSITE BEAMS

E. Graciani[a*], A. Blázquez[a], J. Cañas[a], F. París[a]

[a]*Escuela Superior de Ingenieros, Gr. Elasticidad y Resistencia de Materiales, Universidad de Sevilla, c/ Camino de los Descubrimientos s/n, 41092 Sevilla, Spain*
**egraciani@us.es*

Keywords: Unfolding failure, composite beams, Finite Element Method, Beam models.

Abstract
Unfolding failure in composites is one of the most complicated to deal with since it does not involve failure of fibers, taking then place at a low nominal load level. The accurate prediction of tresses becomes a key factor in designing structural parts susceptible of suffering this kind of failure. Stresses responsible for unfolding failure in a composite T joint are evaluated analytically using a curved beam model. Results are compared with those obtained with a plane finite element model. Analytical and numerical models yield very similar results, being both very conservative if compared with experimental results

1. Introduction

Due to their low specific mechanical properties, composite materials are increasingly employed in aeronautical structures. For this reason, composite components in aeronautical structures are sometimes subjected to complicated loads for which failure criteria have not been specifically developed.

The present study deals with the failure of an aeronautical structure which entails several sandwich panels, sketched in Fig. 1(a), joined together using a frame of composite beams, see Fig. 1(b), the complete structure is hung from the joints of the composite beams, see Fig. 1(c). Although, for the sake of simplicity, flat sandwich panels and composite beams have been depicted in Fig. 1, the real structure is formed by curved panels and beams. However, curvature of the structure is not relevant in the study carried out.

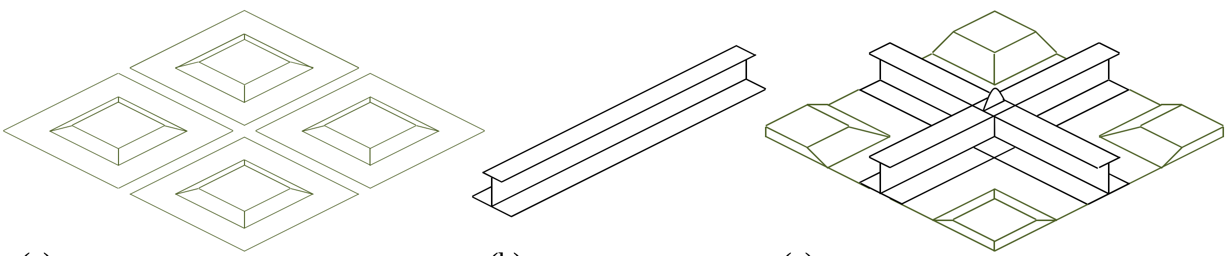

(a) (b) (c)

Figure 1. Joining of sandwich panels with composite beams: (a) sandwich panels, (b) composite beams, (c) detail of the mounted component.

Panels are subjected to pressure loads, which are transmitted through the composite beams to the fixing points. A detail of the joint between sandwich panels and a composite beam is shown in Fig. 2. As can be seen, the foot of the composite beam is bolted to the sandwich panels, and load is transferred through the curved part of the beam, thus creating a complicated stress field in this zone which is subjected to relatively high out-of-plane stresses.

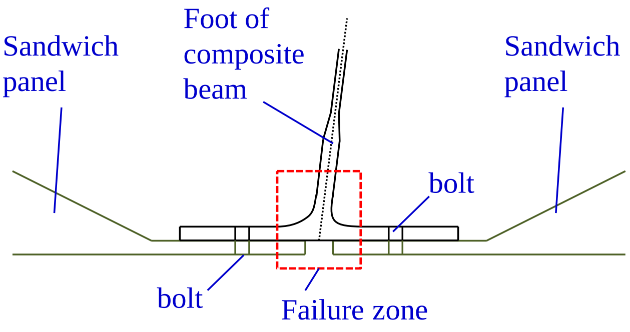

Figure 2. Detail of the T-joint formed by the sandwich panels and the composite beams.

The main objective of this study is developing a methodology for the design of this kind of composite beams, taking into account the unfolding failure [1] in their foot. To this end, simplified analytical models based on Beam Theory have been developed (and compared with 2D FEM models) to evaluate the unfolding stresses in the failure zone depicted in Fig. 2.

2. Problem under study

The problem under study is a typical section of the foot of one of the abovementioned composite beams. As can be seen in Fig. 3(a), beam web is typically reinforced in the foot zone, and a foot reinforcement is also added.

The empty space created between the curved laminates and the foot reinforcement (roving) is filled with unidirectional fibers oriented parallel to the beam axis, that is, perpendicular to the cross section depicted in Fig. 3(a).

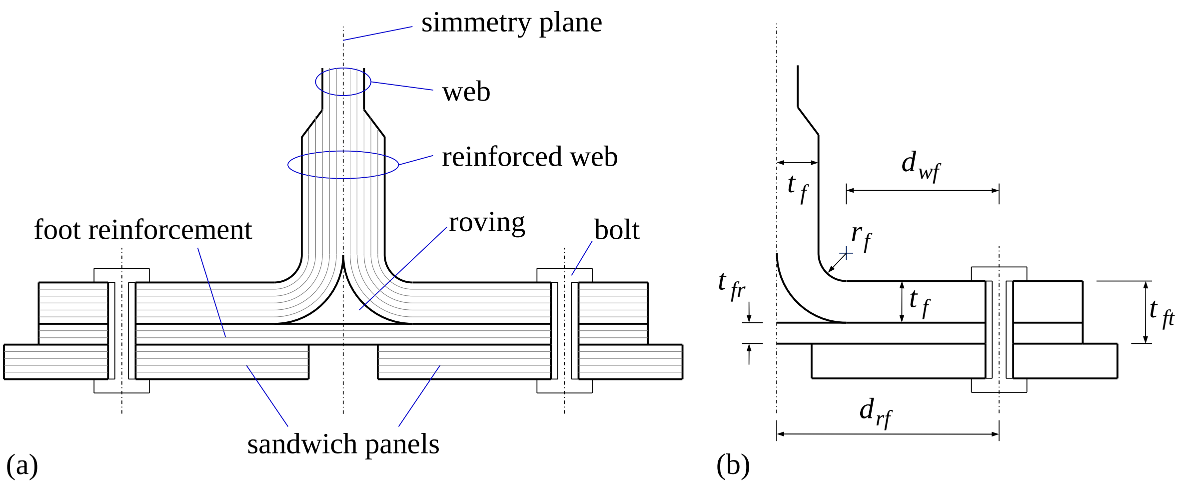

Figure 3. Joint under study: (a) description of the main parts, (b) dimensions.

Characteristic dimensions of the joint are defined in Fig. 3(b). Limited details of the actual configurations employed will be presented for confidentiality reasons.

3. Failure criteria

The following criteria has been employed to determine the unfolding failure of the joint [2,3]:

$$\sqrt{\left(\frac{\sigma_{33}}{\sigma_{33}^{all}}\right)^2 + \left(\frac{\tau_{13}}{\tau_{13}^{all}}\right)^2} \leq 1 \tag{1}$$

were σ_{33} and τ_{13} are the normal and shear unfolding stresses, respectively (see Fig. 4). σ_{33}^{all} and τ_{13}^{all} are the allowable values of σ_{33} and τ_{13}, respectively.

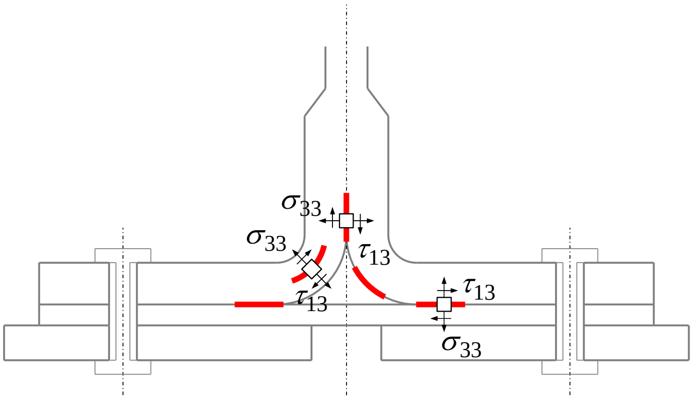

Figure 4. Typical failure locations and unfolding stresses involved in the failure criteria employed.

For the material employed in the study $\tau_{13}^{all} = 61\,\text{MPa}$. The value of σ_{33}^{all} depends on the sign of σ_{33} and the thickness, t, of the laminate. $\sigma_{33}^{all} = 205\,\text{MPa}$ for compressive values of σ_{33}. For tensile values of σ_{33}, the following allowable values have been employed: $\sigma_{33}^{all} = 8.2\,\text{MPa}$ if $t \leq 1\,\text{mm}$, $\sigma_{33}^{all} = 26\,\text{MPa}$ if $t \geq 3\,\text{mm}$ and a linear interpolation between these values if $1\,\text{mm} \leq t \leq 3\,\text{mm}$.

It has to be pointed out that the allowable values of σ_{33} and τ_{13} have been obtained from test of flat or L-shaped laminates, the applicability of these values to the present configuration being under research.

4. Experimental results

The configuration considered in this study correspond to actual samples tested in tension. The test configuration is depicted in Fig. 5, where some of the relevant dimensions and the laminates employed in each part of the foot of the composite beam are also indicated.

The T-shaped sample is clamped in the reinforced web zone, and bolted to a test rig in the foot flanges. Samples of two different lengths (having 25mm and 50mm in the direction perpendicular to the cross section shown in Fig. 5) have been tested.

Only two bolts (one at each side) were employed to fix the sample in the foot flanges. From the test configuration described, it is evident that the stress state in the sample during the test is highly complicated and a 3D study is required to determine properly the failure loads.

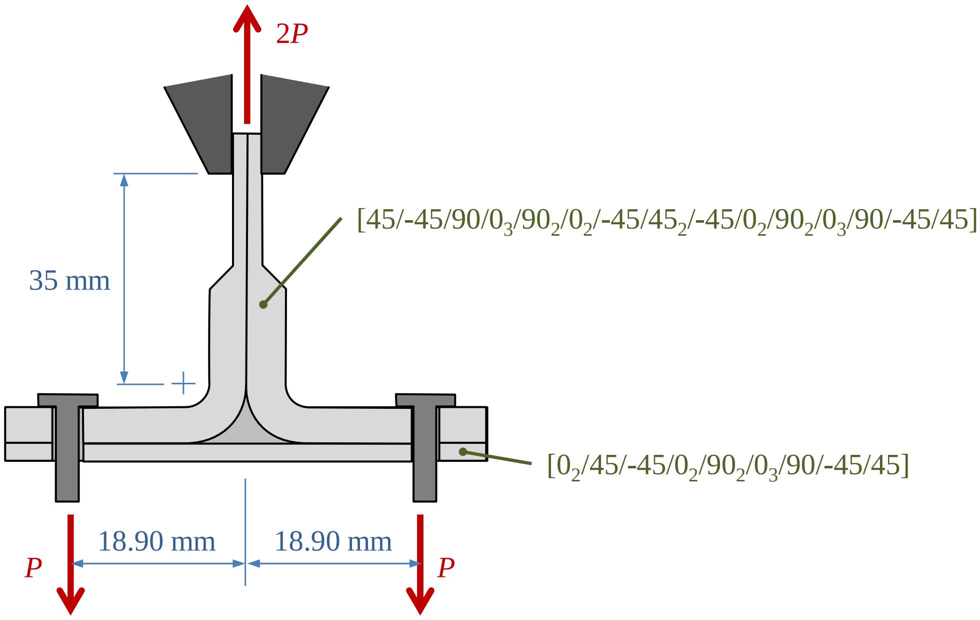

Figure 5. Test configuration and main sample dimensions.

In this study, 2D FEM and 1D analytical analysis have been employed. Experimental results are only treated as a reference for defining the sample configuration, the objective of the paper being the comparison between the 2D FEM model and the 1D analytical model.

5. Analytical models

In order to obtain an analytical solution for the unfolding stresses a simplified beam model has been employed. The main hypotheses carried out in the analytical model are:

- Symmetry of the joint and loads with respect to the symmetry plane shown in Fig. 3 (notice that although the geometry is symmetric, a certain lack of symmetry is derived from the employment of ±45 layers).
- Only the curved zone of the joint and the foot reinforcement under it are considered in the model (see Fig. 6) and the contribution of the roving is neglected.
- Equivalent homogeneous materials are employed to model the laminates.

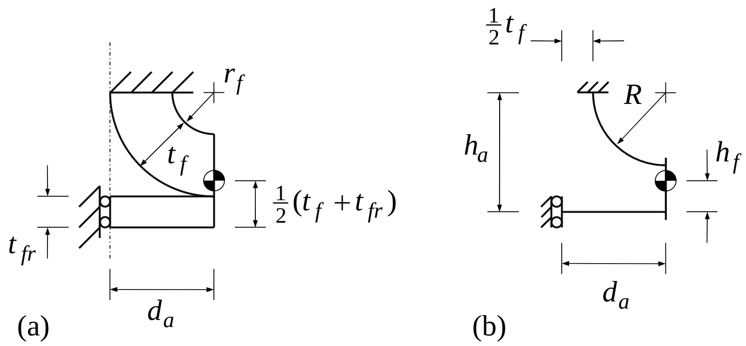

Figure 6. Analytical models: (a) detail of the curved part of the real section of the samples, (b) beam model.

Loads acting in the model are depicted in Fig. 7(a). Loads $F_x^{'}$, $F_y^{'}$ and $M_z^{'}$ are obtained from the load applied during the test (see Fig. 5). Loads P_w, V_w and M_w transmitted to the web and loads P_s and M_s transmitted through the foot reinforcement can be easily computed using beam analysis.

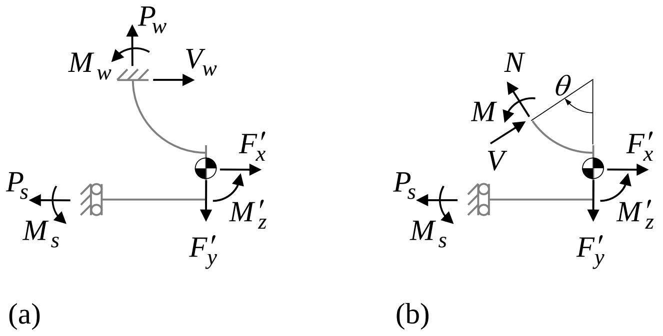

Figure 7. Loads in the analytical models: (a) applied loads and constraint loads, (b) axial and shear loads and bending moment along the curved zone of the beam.

Once the loads at the constraints have been determined, axial and shear forces and bending moment (respectively P, V and M) transmitted through the curved part of the laminate can be obtained as functions of θ angle, defined in Fig 7(b). Unfolding stresses σ_{33} and τ_{13} are determined from $P(\theta)$, $V(\theta)$ and $M(\theta)$, using Lekhnitskii's analytical solution [4].

Two different analytical models have been carried out, the differences being detailed in the next subsections.

4.1. Analytical model A (coupled constitutive equations)

In the first analytical model, shear strains and stresses are considered to vary in a quadratic manner in the laminate, following the law defined by

$$F(z) = \left[1 - \left(\frac{2z}{t}\right)^2\right] \tag{2}$$

with t being the laminate thickness and z a local coordinate in the thickness direction, variying in the range $-\frac{1}{2}t \le z \le \frac{1}{2}t$.

According to the previous hypothesis the following behavior law is obtained for the laminate

$$\begin{Bmatrix} N \\ M \\ V \end{Bmatrix} = \begin{pmatrix} A & B & 0 \\ B & D & 0 \\ 0 & 0 & C \end{pmatrix} \begin{Bmatrix} e_n \\ e_m \\ e_v \end{Bmatrix} \quad , \quad \begin{Bmatrix} e_n \\ e_m \\ e_v \end{Bmatrix} = \begin{pmatrix} E_n & E_{mn} & 0 \\ E_{mn} & E_m & 0 \\ 0 & 0 & E_v \end{pmatrix} \begin{Bmatrix} N \\ M \\ V \end{Bmatrix} \tag{3}$$

Stiffness constants A, B, C and D can be obtained from

$$A = \sum_{i=1}^{n} [Q_N^i (z_i - z_{i-1})] \tag{4}$$

$$B = \tfrac{1}{2} \sum_{i=1}^{n} [Q_N^i (z_i^2 - z_{i-1}^2)] \tag{5}$$

$$D = \tfrac{1}{3} \sum_{i=1}^{n} [Q_N^i (z_i^3 - z_{i-1}^3)] \tag{6}$$

$$C = \frac{5}{4} \sum_{i=1}^{n} \left[Q_V^i \left((z_i - z_{i-1}) - \frac{4}{3t^2} (z_i^3 - z_{i-1}^3) \right) \right] \tag{7}$$

where Q_N^i and Q_V^i can be obtained from the stiffness properties of each lamina:

$$Q_N^i = Q_{11} \cos^4 \alpha_i + 2(Q_{12} + 2Q_{66}) \sin^2 \alpha_i \cos^2 \alpha_i + Q_{22} \sin^4 \alpha_i \tag{8}$$

$$Q_V^i = Q_{55} \cos^4 \alpha_i + Q_{44} \sin^4 \alpha_i \tag{9}$$

with α_i being the orientation of each lamina.

Stiffness constants Q_{11}, Q_{22}, Q_{12}, Q_{44}, Q_{55} and Q_{66} are defined by

$$Q_{11} = \frac{E_{22}}{1 - \nu_{12}\nu_{21}},\ Q_{22} = \frac{E_{11}}{E_{22}} Q_{11},\ Q_{12} = \nu_{12} Q_{22},\ Q_{44} = Q_{55} = \frac{E_{22}}{2},\ Q_{66} = G_{12} \tag{10}$$

Notice that $\alpha = 0$ is the longitudinal direction of the composite beam (i.e. the direction perpendicular to the cross section shown in Fig. 5).

4.2. Analytical model B (uncoupled constitutive equations)

In the second analytical model, coupling between axial and bending strains is neglected and, therefore, the following behavior law is obtained for the laminate

$$\begin{Bmatrix} e_n \\ e_m \\ e_v \end{Bmatrix} = \begin{pmatrix} E_n & 0 & 0 \\ 0 & E_m & 0 \\ 0 & 0 & E_v \end{pmatrix} \begin{Bmatrix} N \\ M \\ V \end{Bmatrix} \tag{11}$$

where E_n, E_m and E_v are evaluated from the expressions shown in the previous subsection.

6. FEM models

The solution obtained with the analytical models have been compared with a 2D FEM model created using MSC.Nastran [5], see Fig. 8(a). Plane stress conditions have been considered in the model. Individual laminas have been model using CQUAD4 elements with appropriate orthotropic material properties.

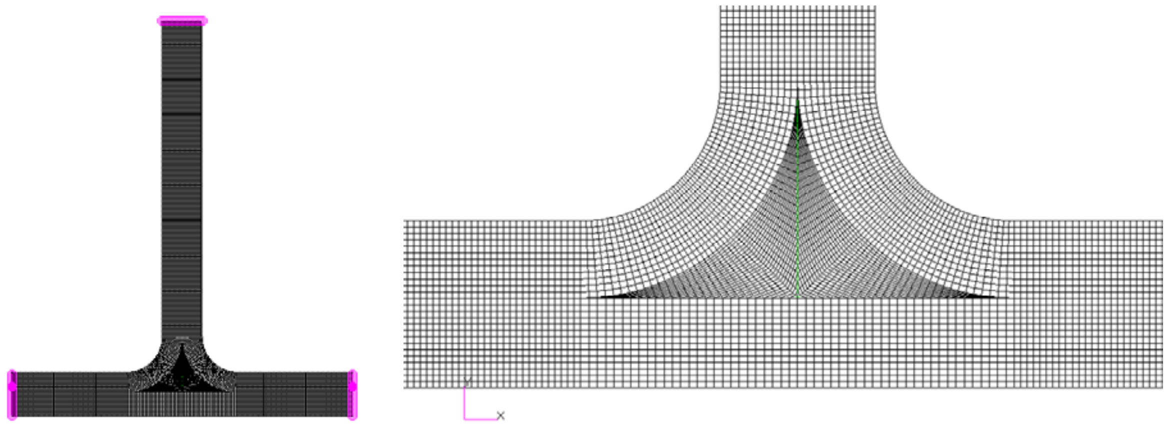

(a) (b)

Figure 8. FEM model: (a) full mesh view, (b) detail of the mesh in the curved zone.

A detail view of the curved zone of the laminates is shown in Fig. 8(b). As can be seen, a single element per lamina in the thickness direction is employed in this model. A mesh refinement (using several elements per lamina in the thickness direction) was carried out in order to obtain a precise solution of unfolding stresses in the curved zone.

7. Results and comparison

For the sample described in Fig. 5, the load P needed to cause unfolding failure has been determined employing the analytical models described in section 5 and the FEM model described in section 6.

In both cases, problem has been solved assuming $P = 1$ N/mm, and the maximum of the expression shown in the left hand side of the failure criteria (1) has been evaluated, thus allowing us to determine the value of the load P needed to cause unfolding failure.

Results obtained are listed in Table 1, in which for the sake of comparison, the failure loads obtained experimentally in two sets of samples have also been included. The first set of samples consisted in 4 samples with 50 mm length, while the second set of samples consisted in 2 samples with 25 mm length.

Analytical (A)	**Analytical (B)**	**FEM 2D**	**Experim. (50 mm)**	**Experim. (25 mm)**
33.8 N/mm	32.9 N/mm	31.8 N/mm	72.7 ± 11.6 N/mm	87.3 ± 14.7 N/mm

Table 1. Failure loads obtained with the models and the experiments.

As can be seen predictions obtained with both analytical models and with the FEM model are quite similar, being all of them very conservative if compared with the experimental results.

8. Concluding remarks

The possibility of applying simplified analytical model to the study of the unfolding failure in composite T-joints has been studied.

Analytical models employ Beam Theory to determine the loads (axial and shear loads and the bending moment) transferred through the curved part of the T-joint and Lekhnitskii's analytical solution to determine the unfolding stresses from these loads.

Results have been compared with the solution of a more detailed 2D FEM model, showing a good agreement in the determination of the failure load of the joint. These results are a promising start in the development of an easy-to-use analytical design tool for this kind of joints.

A more detailed study, using different configurations with different web laminates and different foot reinforcements should be carried out to determine the range of applicability of the developed analytical models.

Both analytical and FEM models yield very conservative results in comparison with the experimental failure loads measured experimentally. These results were expected since the influence of 3D effects was neglected in the analysis and the allowable values of σ_{33} and τ_{13} may not be directly applied to the configuration under study.

References

[1] E. E. Theotokoglou and T. Moan. Experimental and numerical study of composite T-joints. *Journal of Composite Materials,* 30:190-209, 1996.
[2] Z. Hashin. Failure criteria for unidirectional composites. *Journal of Applied Mechanics*, 47:329-334, 1980.
[3] R. Y. Kim and S. R. Soni. Failure of composite laminates due to combined interlaminar normal and shear stresses. In *Composites'86*, pages 341-50, 1986.
[4] S. G. Lekhnitskii. *Theory of Elasticity of an Anisotropic Body*, MIR Publishers, Moscow, 1981.
[5] MSC.Software Corporation. *MSC.Nastran 2005 r3. Quick Reference Guide*, 2006